



NUMERICAL MODELING OF GPR FIELD IN DAMAGE DETECTION OF A REINFORCED CONCRETE FOOTBRIDGE

Jacek LACHOWICZ, Magdalena RUCKA

Gdańsk University of Technology, Faculty of Civil and Environmental Engineering,
Department of Mechanics of Materials and Structures,
Ul. Narutowicza 11/12, 80-233 Gdańsk, Poland, e-mail: jaclacho@pg.gda.pl, mrucka@pg.gda.pl

Summary

The paper presents a study on the use of the ground penetrating radar (GPR) method in diagnostics of a footbridge. It contains experimental investigations and numerical analyses of the electromagnetic field propagation using the finite difference time domain method (FDTD). The object of research was a reinforced concrete footbridge over a railway line. The calculations of the GPR field propagation were performed on a selected cross-section of the bridge. Three different damage scenarios (i.e. one missing rebar and two air voids with different shapes and locations) were investigated in FDTD simulations. Numerical GPR maps were compared with results of in-situ GPR surveys for the healthy footbridge.

Keywords: damage detection, ground penetrating radar method, FDTD simulations.

NUMERYCZNE MODELOWANIE POLA GEORADAROWEGO W DETEKCJI USZKODZEŃ ŻELBETOWEJ KŁADKI DLA PIESZYCH

Streszczenie

W artykule przedstawiono użycie metody georadarowej w procesie diagnostyki kładki dla pieszych. Praca zawiera badania doświadczalne oraz analizy numeryczne propagacji pola elektromagnetycznego z wykorzystaniem metody różnic skończonych w dziedzinie czasu. Przedmiotem badań była żelbetowa kładka dla pieszych usytuowana nad torami kolejowymi. Obliczenia wykonano na przykładzie wybranego przekroju poprzecznego kładki. Rozważono trzy różne scenariusze uszkodzeń, tj. brak jednego z prętów zbrojeniowych oraz dwie pustki powietrzne o różnych kształtach i lokalizacjach. Wyniki symulacji porównano z wynikami badań doświadczalnych przeprowadzonych na nowo wybudowanym obiekcie.

Słowa kluczowe: wykrywanie uszkodzeń, metoda georadarowa, obliczenia metodą różnic skończonych.

1. INTRODUCTION

The ground penetrating radar (GPR) method has been widely used as one of the most powerful methods directed to non-destructive evaluation of geological media as well as engineering structures [1-2]. It is commonly used for in-situ diagnostics of bridges [3], roads [4], reinforced concrete [5] and masonry structures [6]. There are many factors which can influence the experimental GPR results, for example material humidity, wave interference from high-voltage lines or metal structures situated near the survey location. Moreover, similar types of patterns in a GPR map can be caused by different types of defects. For this reason, the interpretation of measurement data is a primary problem in the GPR technique. Recently, the use of numerical modelling with the use of the finite difference time domain (FDTD) method has become a powerful support for understanding electromagnetic field propagation in complex structures [7-11]. Results of numerical simulations can be useful in explaining the origin of reflections appearing in GPR experimental data or in

creation of a base of GPR maps with different damage scenarios for an automated structural health monitoring system.

This study aims to the interpretation of the radargrams with the use of numerical models of the GPR field using the finite difference time domain method. Investigations were carried out for a cross-section of a footbridge. Three different damage scenarios in the form of one missing rebar and two air voids with different shapes and locations were investigated in FDTD simulations. Numerical GPR maps were compared with results of in-situ GPR surveys for the healthy footbridge.

2. THEORETICAL BACKGROUND OF NUMERICAL MODELING OF GPR FIELD

The Maxwell's equations describing the properties of magnetic and electric fields and the relationships between them are the theoretical basis of the propagation of electromagnetic waves. The Maxwell's equations in anisotropic and lossy media take the form [11]:

$$\nabla \times \mathbf{E} = -\frac{\partial \mathbf{B}}{\partial t}, \quad (1)$$

$$\nabla \times \mathbf{H} = \frac{\partial \mathbf{D}}{\partial t} + \mathbf{J}_c + \mathbf{J}_s, \quad (2)$$

$$\nabla \cdot \mathbf{B} = 0, \quad (3)$$

$$\nabla \cdot \mathbf{D} = q_v, \quad (4)$$

where \mathbf{B} is the magnetic flux density vector, \mathbf{D} – the electric displacement vector, \mathbf{E} and \mathbf{H} – the electric and magnetic field strength vectors, respectively, \mathbf{J}_s – the impressed current density, \mathbf{J}_c – the conduction current density, t – time and q_v – the volume electric charge density.

In order to calculate the propagation of the GPR field, equations (1-4) should be solved with given boundary conditions. Due to the fact that the analytical solution of these equations is very difficult, the numerical methods became popular. One of such methods is proposed in 1966 by Yee, the finite difference time domain method [12]. In this approach, a continuous model is converted into a discrete one. The material properties are assigned in nodes of Yee cells, while the components of electric and magnetic fields are calculated in a leapfrog manner. This process is fully explicit, completely getting rid of the problem of solving simultaneous equations and matrix inversion. A scheme of two-dimensional Yee grid at a selected instant of time is shown in Fig. 1.

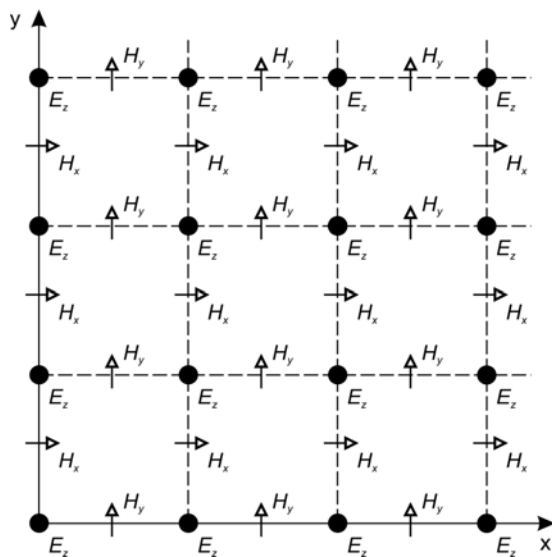


Fig. 1. Scheme of two-dimensional Yee grid at selected instant of time

Derivatives are approximated using finite differences according to the formula:

$$\frac{\partial F}{\partial x} \approx \frac{F_{i+1,j} - F_{i,j}}{\Delta x}, \quad (5)$$

$$\frac{\partial^2 F}{\partial x^2} \approx \frac{F_{i+1,j} - 2F_{i,j} + F_{i-1,j}}{(\Delta x)^2}, \quad (6)$$

where F is a considered function, i, j – numbering grid nodes, Δx – the mesh size of the Yee grid.

Simplifying the Maxwell's equations to two dimensions for the transverse electromagnetic TM_z mode, in which the H_z , E_x and E_y components of the electromagnetic fields are zero, we get the equations incorporating the H_x , H_y and E_z components perpendicular to each other:

$$\mu \frac{\partial H_x}{\partial t} = -\frac{\partial E_z}{\partial y}, \quad (7)$$

$$\mu \frac{\partial H_y}{\partial t} = \frac{\partial E_z}{\partial x}, \quad (8)$$

$$\varepsilon \frac{\partial E_z}{\partial t} = \frac{\partial H_y}{\partial x} - \frac{\partial H_x}{\partial y}, \quad (9)$$

where ε denotes the dielectric constant and μ is the magnetic permeability.

The general scheme of the two-dimensional computational model of the FDTD method is shown in Fig. 2. In order to excite an impulse wave imitating the signal emitted from the antenna during GPR measurements, the source of the wave is introduced at selected nodes of the Yee cell. The currents vectors are specified at successive time instants by an appropriate mathematical function. The receiving antenna is introduced through recording the signal in one of the grid nodes. In order to prevent the reflections of propagating waves from boundaries of the computational model, absorbing boundary conditions (ABC) are applied.

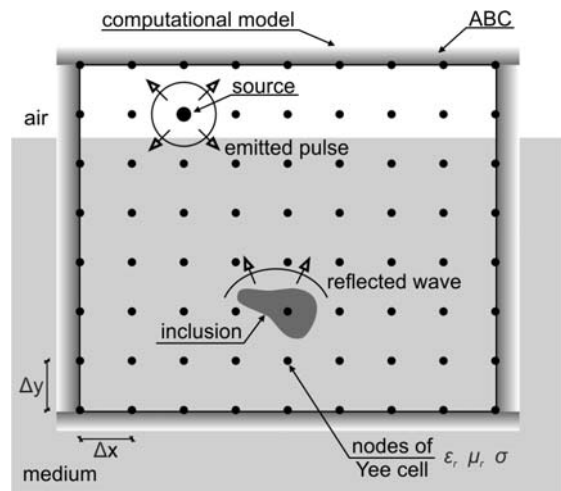


Fig. 2. General scheme of two-dimensional model of FDTD method

3. OBJECT OF INVESTIGATIONS

Numerical and experimental investigations were carried out on a cross section of the footbridge KL-19 (Fig. 3) built within walking route over the line of the Pomeranian Metropolitan Railway in Gdańsk. The bridge is a frame arch structure with a theoretical span of 28 m. The single girder arch is firmly established in continuous footings. The deck plate with a constant thickness of 50 cm is based on the abutments, and is connected monolithically in the arch crown. The surface of the bridge deck is covered with epoxy resin.

4. NUMERICAL ANALYSIS BY FDTD METHOD

The basic model subjected to analysis of the electromagnetic wave propagation was the cross-section of the intact footbridge, with the layouts and dimensions of the reinforcement applied in accordance with the technical documentation (Fig. 4a). Additionally, three models with different damage scenarios were considered. In the first damage scenario one of the rebar was removed (Fig. 4b). The second and the third damage scenario contained air voids. The rectangular void with

dimensions 200 mm \times 20 mm and the circular void with a diameter of 40 mm were introduced at positions indicated in Fig. 4c and Fig. 4d, respectively.

The calculations were performed using the software called GprMax 2D [11]. The two-dimensional models were discretized into cells with dimensions 1 mm \times 1 mm. The following parameters were established: $\epsilon_r = 9$, $\sigma = 0.01$ S/m (for concrete) and $\epsilon_r = 1$, $\sigma = 10^7$ S/m (for steel). As an excitation signal the Ricker function with a frequency of 2 GHz was used due to its high compatibility with the signal emitted by the radar antenna.



Fig. 3. Footbridge KL-19

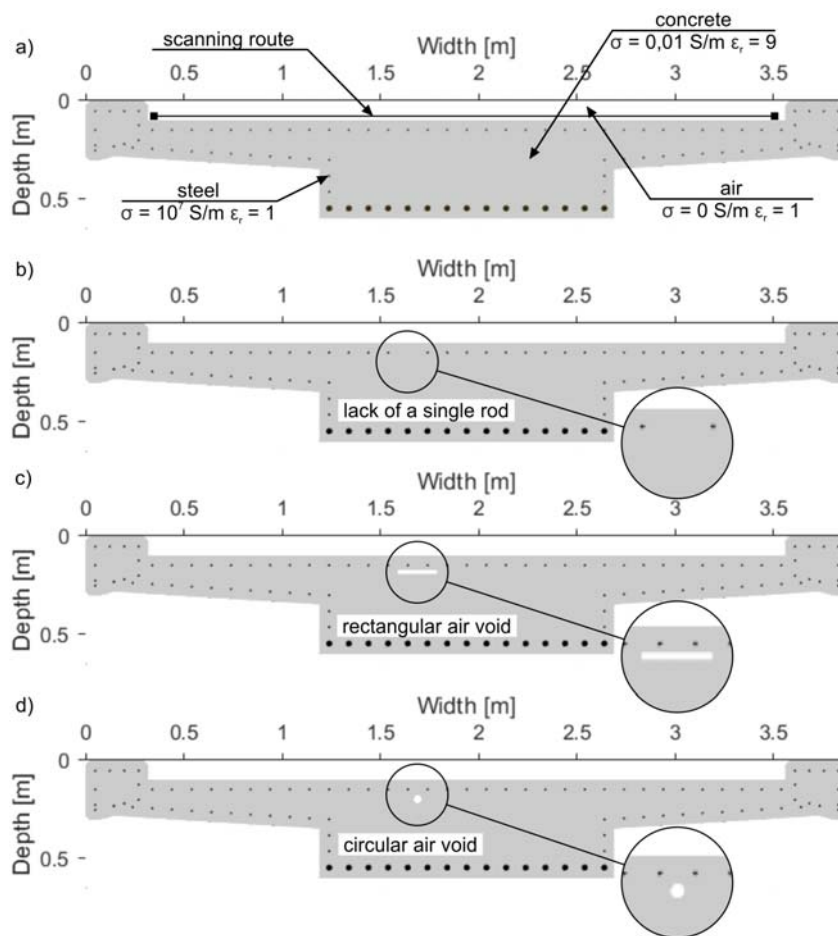


Fig. 4. Numerical models of the footbridge cross-section: a) without damage; b) with one rebar removed; c) with the rectangular air void; d) with the circular air void

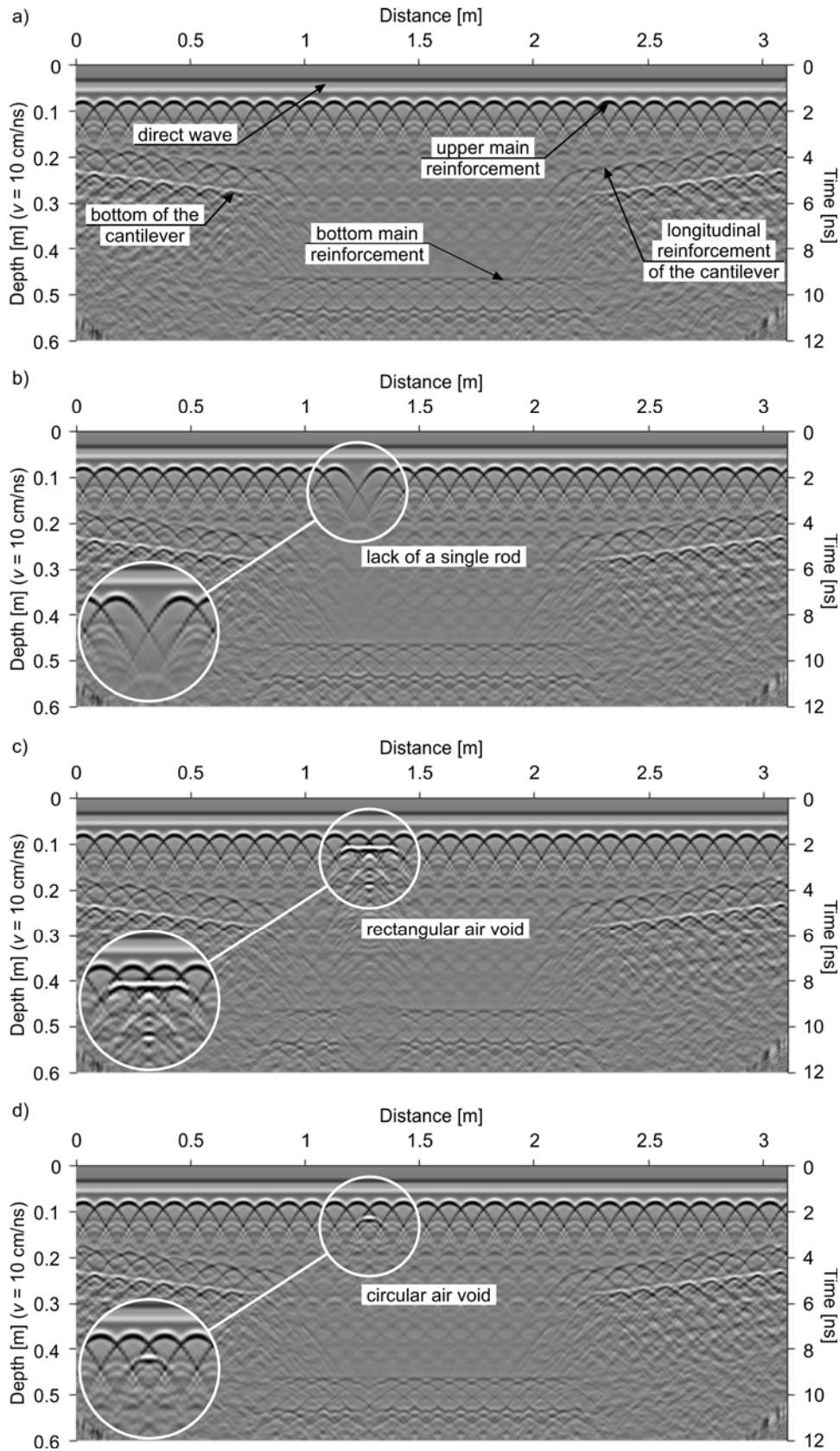


Fig. 5. Results of FDTD simulations of georadar field propagation through the footbridge cross-section: a) without damage; b) with one rebar removed; c) with the rectangular air void; d) with the circular air void

Figure 5a shows the results of FDTD simulations for the footbridge cross-section in the intact state, in the form of GPR maps called radargrams. In the GPR maps three rows of hyperbola patterns are visible. They correspond to reflections from the upper and the bottom main reinforcement as well as the reinforcement of the cantilever part of the girder. The positions of hyperbolas allow specifying the number and the position of rebars. An individual steel bar is located in the vertex of a hyperbola. Moreover, wave reflections from the external edges of the structure enable estimation of the geometry of the footbridge cross-section.

In the case, when there is a lack of one of the steel bars, on the GPR maps one hyperbola is missing (Fig 5b). This type of defect can be detected by analysing the repetition of reflection patterns of hyperbolas. Results for the bridge with air void defects are shown in Fig. 5c and Fig. 5d. Such voids can appear as a result of inappropriate concrete manufacturing process. In both GPR maps (Fig. 5c and Fig. 5d) additional reflections are visible near the position of damage. The rectangular damage is characterized on the radargram by a longitudinal reflection from the top of the void and hyperbolic closure at each end. The circular air gap caused a single hyperbolic reflection, but with different pattern than in the case of the reflection from a steel bar.

5. EXPERIMENTAL INVESTIGATIONS

Experimental investigations were carried out using a GPR Aladdin system, which consists of a bipolar antenna with an operating frequency of 2 GHz, the control unit, the portable computer and

the battery. Several transversal measurements were taken along the width of the footbridge deck, at selected locations depicted in Fig. 6.

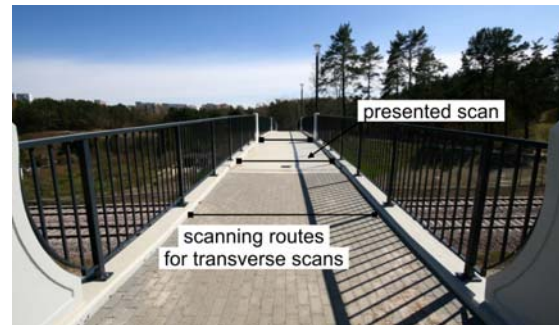


Fig. 6. GPR surveys on the footbridge with selected routes for transversal scanning

Figure 7 shows the processed GPR map acquired between footing and the arch crown, superimposed on the cross-section of the structure. The upper row of the main reinforcement rods in an average spacing of 10 cm and the lower row of the longitudinal reinforcement of the cantilever part of the girder in the same spacing are clearly visible. Due to the fact that the noise level begins at a depth of approximately 45 cm, the lower reinforcement of the deck was not detected. Additionally, on the lower areas of the radargram noise from outer metal parts, probably the handrail, is visible in the form of diagonal patterns. Any anomalies that could indicate a presence of structural damage were not detected. Analyzing the reproducibility of reflections from the reinforcement, there was no lack of a rebar.

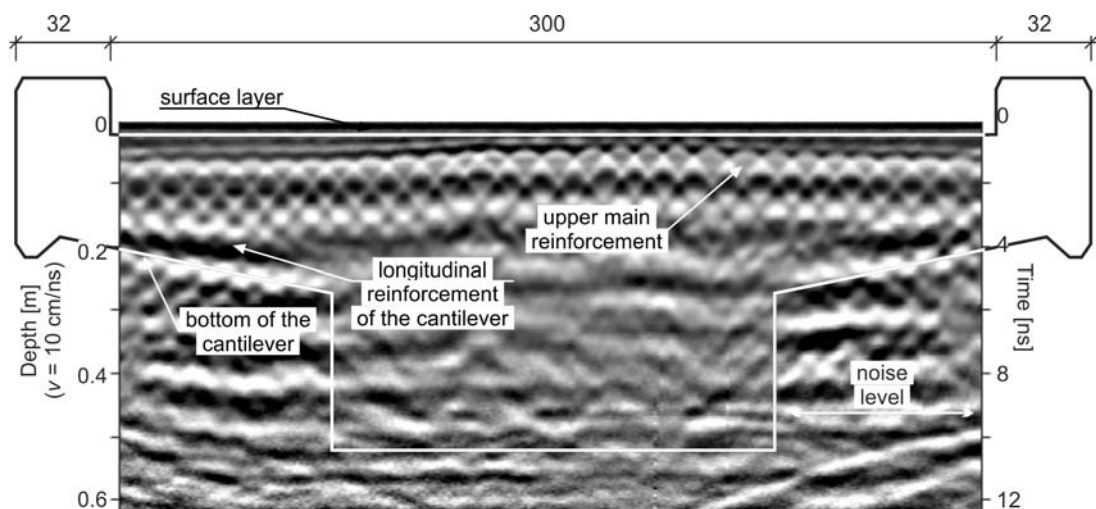


Fig. 7. GPR map obtained from in-situ surveys superimposed on the footbridge cross-section

6. CONCLUSIONS

In this paper the application of the ground penetrating radar method in non-destructive diagnostics of the reinforced concrete footbridge was presented. The experimental in-situ

measurements conducted on the newly built footbridge were supported by numerical modelling of the GPR field using the finite difference time domain method. The numerical analyses were performed on the cross-section of the bridge in the healthy stage and for three damage scenarios which



included one missing rebar, one circular air void and one rectangular air void. Numerical GPR maps for the structure without damage were compared with results of in-situ GPR surveys. The radargrams for the intact structure allowed determining the distribution and amount of reinforcement in the cross-section of the footbridge. Numerical studies on the damaged structures have shown that by analyzing the repetition of reflections the lack of a rebar can be detected. Air voids generated different reflections depending on their shapes. The circular air gap caused a single hyperbolic reflection, but with different pattern than in the case of the reflection from a reinforcement bar due to different diameter. In the case of the rectangular void, the strong longitudinal reflection with two hyperbolic closures at each ends was identified. The results of numerical simulations showed the usefulness of the GPR field modelling for enhancing the understanding of damage detection schemes that may occur during the operation of the structure.

REFERENCES

1. Karczewski J, Ortyl Ł, Pasternak M. Zarys metody georadarowej. Wydawnictwa AGH, Kraków; 2011. Polish.
2. Gołębiowski T. Zastosowanie metody georadarowej do detekcji i monitoringu obiektów o stochastycznym rozkładzie w ośrodku geologicznym. Wydawnictwa AGH, Kraków; 2012. Polish.
3. Bęben D, Mordak A, Anigacz W. Ground penetrating radar application to testing of reinforced concrete beams. *Procedia Engineering*. 2013;65:242-247.
4. Saarenketo T, Scullion T. Road evaluation with ground penetrating radar. *Journal of Applied Geophysics*. 2000;43:119-138.
5. Lachowicz J, Rucka M. Application of GPR method in diagnostics of reinforced concrete structures. *Diagnostyka*. 2015;16(2):31-36.
6. Binda L, Zanzi L, Lualdi M, Condoleo P. The use of georadar to assess damage to a masonry Bell Tower in Cremona, Italy. *NDT&E International*. 2005;38:171-179.
7. Diamanti N, Giannopoulos A, Forde MC. Numerical modelling and experimental verification of GPR to investigate ring separation in brick masonry arch bridges. *NDT&E International*. 2008;41:354-363.
8. Hamrouche R, Kłysz G, Balayssac JP, Rhazi J, Ballivy G. Simulation and detection limit of EM waves in masonry structures with an algorithm for

image processing. *Progress in Electromagnetics Research Symposium Proceedings*. Marrakesh, Marocco. 2011:1799-1803.

9. Gołębiowski T. Wprowadzenie do metodyki interpretacji badań georadarowych przy użyciu procedury modelowania numerycznego. *Przegląd Geologiczny*. 2004;7:563-568. Polish.
10. Solla M, Lorenzo H, Novo A, Caamaño J C. Structural analysis of the Roman Bibei bridge (Spain) based on GPR data and numerical modelling. *Automation in Construction*. 2012; 22:334-339.
11. Giannopoulos A. Modelling ground penetrating radar by GprMax. *Construction and Building Materials*. 2005;19(10):755-762.
12. Yee K S. Numerical solution of initial boundary value problems involving Maxwell's equations in isotropic media. *IEEE Transactions on Antennas and Propagation*. 1966;14:585-589.

Received 2016-02-08

Accepted 2016-02-23

Available online 2016-06-04



Jacek LACHOWICZ, M.Sc. graduated civil engineering at the Department of Mechanics of Materials and Structures of Gdańsk University of Technology. Since October 2014 he continues his education as a Ph.D. student. He mainly deals with GPR diagnostic method.



Magdalena RUCKA, Ph.D., D.Sc. is an assistant professor at the Department of Mechanics of Materials and Structures of Gdańsk University of Technology. Her scientific interests are focused on dynamic of structures, wave propagation and development of new techniques for damage detection and structural health monitoring.